The Journal of Experimental Biology 210, 311-324
Published by The Company of Biologists 2007
doi:10.1242/jeb.02646

The predictive start of hunting archer fish: a flexible and precise motor pattern performed with the kinematics of an escape C-start

Saskia Wöhl and Stefan Schuster*

Universität Erlangen-Nürnberg, Institut für Zoologie II, Staudtstrasse 5, D-91058 Erlangen, Germany

*Author for correspondence (e-mail: sschuste@biologie.uni-erlangen.de)

Accepted 9 November 2006

Summary

Once their shots have successfully dislodged aerial prey, hunting archer fish monitor the initial values of their prey's ballistic motion and elicit an adapted rapid turning maneuver. This allows these fish to head straight towards the later point of catch with a speed matched to the distance to be covered. To make the catch despite severe competition the fish must quickly and yet precisely match their turn and take-off speed to the initial values of prey motion. However, the initial variables vary over broad ranges and can be determined only after prey is dislodged. Therefore, the underlying neuronal circuitry must be able to drive a maneuver that combines a high degree of precision and flexibility at top speed. To narrow down which neuronal substrate underlies the performance we characterized the kinematics of archer fish predictive starts using digital high-speed video. Strikingly, the predictive starts show all hallmarks of Mauthner-driven teleost C-type fast-starts, which have previously not been noted in feeding strikes and were not expected to provide the high angular accuracy required. The high demands on flexibility and precision of the predictive starts do not compromise their performance. On the contrary, archer fish predictive starts are among the fastest C-starts known so far among teleost fish, with peak linear speed beyond 20 body lengths s^{-1}, angular speed over 4500 deg. s^{-1}, maximum linear acceleration of up to 12 times gravitational acceleration and peak angular acceleration of more than 450 000 deg. s^{-2}. Moreover, they were not slower than archer fish escape C-starts, elicited in the same individuals. Rather, both escapes and predictive starts follow an identical temporal pattern and all kinematic variables of the two patterns overlap. This kinematic equivalence strongly suggests that archer fish recruit their C-start escape network of identified reticulospinal neurons, or elements of it, to drive their predictive starts. How the network drives such a rather complex behavior without compromising speed is a wide open question.

Key words: sensorimotor integration, reticulospinal system, C-start, fast-start, prediction, cognition, fish, archer fish.

Introduction

When a split second decides between life and death, both hunters and their prey produce distinct high-speed motor patterns at their limits of performance. One of the best-studied is the so-called C-type start of escaping teleost fish. In this two-stage motor program a fish turns and attains high acceleration by first bending its body into a C-shape and then straightening it, thus pushing off water with the full broadside of its body (Weihs, 1973; Webb, 1975). Numerous neurophysiological and neuroethological studies (reviewed in Faber et al., 1989; Nissanov and Eaton, 1989; Domenici and Blake, 1997; Zottoli and Faber, 2000; Eaton et al., 2001; Hale et al., 2002; Fetcho and Bhatt, 2004) have contributed to making the underlying network of identified reticulospinal neurons perhaps the best approachable vertebrate model system for sensorimotor integration. The escape network of fish has been studied with a wide range of techniques, from chronic recordings in the behaving animal (e.g. Zottoli, 1977; Deliagina et al., 2000) to a steadily increasing wealth of novel optical and genetic techniques (Fetcho and O'Malley, 1997; O'Malley et al., 1996; Fetcho and Bhatt, 2004; Fetcho and Higashijima, 2004; Hale et al., 2004; Miesenböck, 2004). Furthermore, although some of the cellular components of the escape network are already found in lamprey (e.g. McClellan and Grillner, 1983; Buchanan, 1993) the network is by no means conservative but appears capable of rapid evolutionary changes (Westneat et al., 1998; Hale et al., 2002; O'Steen et al., 2002; Tytell and Lauder, 2002).

Previously, C-starts were not noticed in precisely aimed feeding strikes (Fig. 1). A reason for this could be that in an escape the purpose is simply to get away from the source of danger, which demands a motor pattern optimized in terms of acceleration but not necessarily in terms of precision (e.g. Bennett, 1984). While several studies have shown that the

mean escape direction can well be set in relation to the direction of a stimulus, the scatter around this mean direction is large (Eaton and Emberley, 1991; Domenici and Blake, 1993; Foreman and Eaton, 1993; Domenici and Blake, 1997; Domenici and Batty, 1997; Tytell and Lauder, 2002) and it is not known whether take-off speed is tunable in escapes. Most importantly, the angular scatter appears too large for these responses to be used to precisely strike at a target over larger distances. Evidently, for an escape a large scatter around a mean direction would seem to be of clear survival advantage: it prevents predators from adjusting to the regularities in their prey's escape pattern. For escapes that require higher precision – for instance when collisions with school members must be avoided – a much slower C-start is used (Domenici and Batty, 1997; Domenici and Blake, 1997). This, again, supports the view that evolution has shaped the fast C-starts to be fast but not very precise. When both top speed and high precision are needed, as in predatory strikes, fish use a kinematically (Webb, 1976; Harper and Blake, 1990; Spierts and van Leeuwen, 1999; Hale, 2002; Schriefer and Hale, 2004) and probably also neuronally (Hale, 2002), different fast-start pattern, the S-type start. In this, the fish's body first bends not into a C but an S-shape. These starts usually do not involve large turns (Domenici and Blake, 1997; Hale, 2002) but are directed in or close to the initial pre-start orientation of the fish. Interestingly, a detailed comparison of S-type escapes and strikes of pike suggests that more complex neuronal circuitry is used to drive the precisely aimed strikes, which require a longer initial bending phase than do the escapes (Schriefer and Hale, 2004).

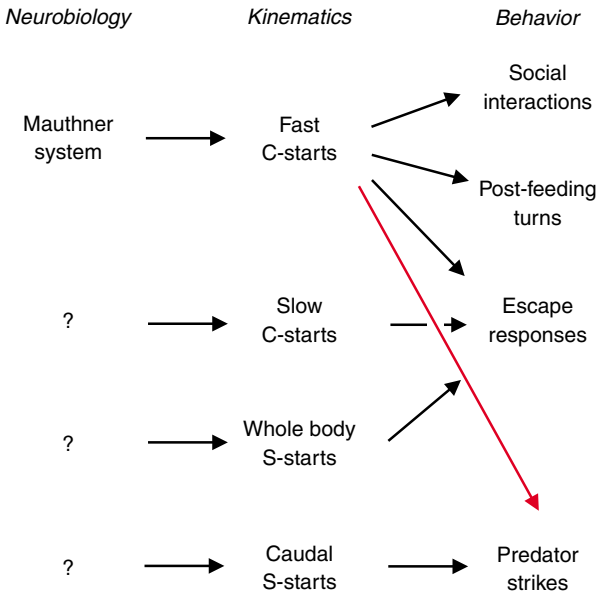

Fig. 1. Diagram based on Domenici and Blake (Domenici and Blake, 1997) and Schriefer and Hale (Schriefer and Hale, 2004) summarizing present knowledge of fast-start motor patterns in fish. The present study provides the first demonstration that fast C-starts, on which most neurobiological work has focussed, can be used in precisely aimed feeding strikes (red arrow). Our findings imply that C-start circuitry can be used to drive rather complex behavior at high precision and top speed.

In summary, all previous evidence suggests that fish use distinct high-speed circuitry optimized to serve distinct purposes: either to (1) rapidly drive large turns, but at compromised precision, or (2) drive precisely aimed starts in a restricted angular range and at lesser performance. Here we provide an example that challenges this view: the predictive start of archer fish.

In their impressive hunting behavior (e.g. Lüling, 1963; Dill, 1977; Schuster et al., 2004; Schuster et al., 2006; Schlegel et al., 2006), archer fish dislodge prey by precisely aimed shots of water and catch and devour their prey as it hits the water surface. Dislodged prey usually attains horizontal speed and falls on a ballistic path towards the water surface. As soon as the prey has started falling, both shooter and bystanding school members can predict the later point of prey impact. A rapid turn aligns them precisely to the later point of catch and the fish take off with a speed matched to the distance they will have to cover (Rossel et al., 2002; Wöhl and Schuster, 2006). The precision of the response (about 6°) is remarkable because the fish must rapidly select turn size and take-off speed from a broad range, based solely on sensory information sampled within less than 100 ms of the prey's motion (Fig. 2). Therefore, the underlying motor network must be able to combine extreme speed with both precision and flexibility. To narrow down our search for the underlying neuronal substrate we studied the kinematics of the predictive starts and compared them both with the wealth of fast start patterns known in other teleost fish (Fig. 1) as well as directly with archer fish fast C-type escapes. Strikingly, the predictive starts of archer fish show all the hallmarks of a fast C-start and are kinematically equivalent to archer fish escape C-starts. Therefore the findings imply that the same elements of reticulospinal circuitry are recruited to drive both motor patterns.

Materials and methods

Fish

A group of six archer fish *Toxotes jaculatrix* Pallas 1767 was kept in a large tank (160 cm×60 cm×60 cm, length×depth×height) filled to 30 cm height with brackish water (temperature 28±1°C, mean ± s.d.; conductivity 3.8–4.0 mS cm^{-1}). The group had been established 2 years prior to this study beginning and all fish readily shot down targets from large heights and competed for dislodged prey. Body length (from snout to caudal peduncle) ranged from 8 to 9 cm (8.6±0.4 cm, mean ± s.d.) and mass was 28–39 g. The stretched-straight center of mass (CM) was determined in three of our experimental fish. While this point is often used as a convenient reference in analysing fish fast-starts, it should be noted that in strongly bent fish it may deviate substantially from the true center of mass. Fish were stretched straight, frozen and the CM determined using plumblines. The stretched-straight CM of archer fish is

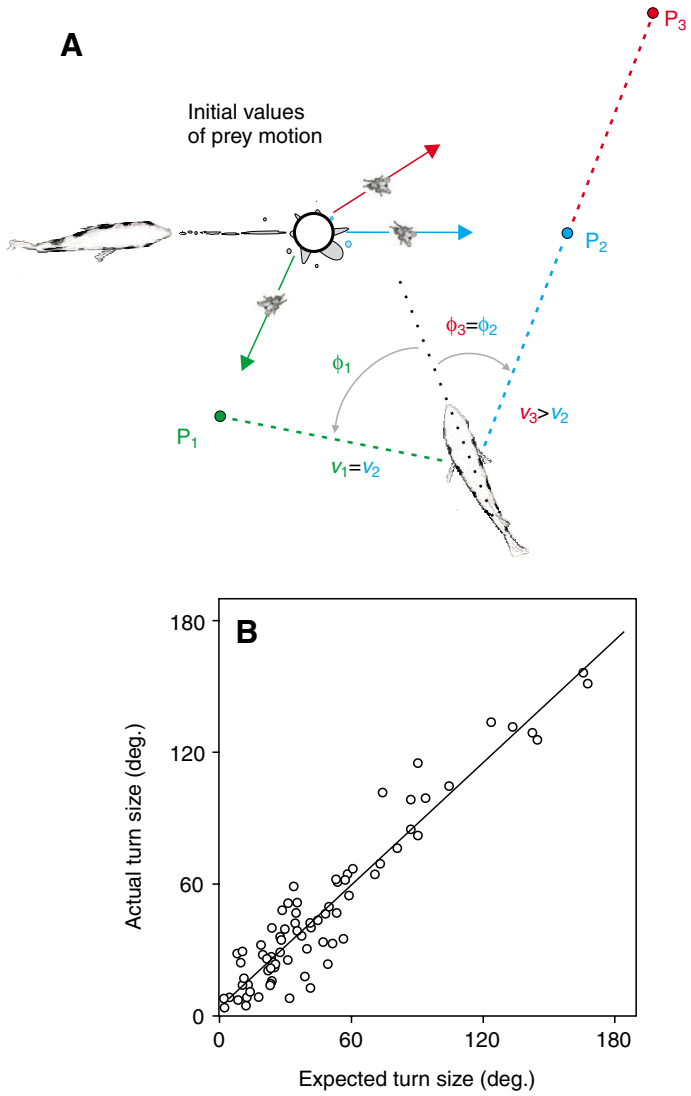

Fig. 2. The predictive start of archer fish. (A) After the shot of a group member has just dislodged an aerial insect, a responding fish (lower right) turns from its initial orientation (dotted line) and takes off directly towards the later point of impact, with a speed matched to distance. Because the initial values of prey motion (initial height, speed and take-off angle) vary independently over broad ranges, predicted points P of impact can be anywhere within a large area. They must be inferred from a quick judgement of the prey's initial motion, based on which the fish must rapidly select an appropriate turn (angle ϕ) and take-off (speed v). The match that the responding fish must make is illustrated by showing three ways (in different colors) in which a given shot might dislodge the target insect. The correspondingly different impact points P_1–P_3 (shown in the respective colors) would require speed levels v_1–v_3 and turning angles ϕ_1–ϕ_3. Responses aimed at P_1 and P_2 would require different turns but the same take-off speed, whereas responses to P_2 and P_3 would require the same turn, but different take-off speed. (B) The actual turning range and accuracy in the set of predictive starts (N=76) whose kinematics are analyzed in this study using digital high-speed video. Turns were accurately set to the later point of impact and accuracy did not decrease when larger turns were required. The regression line (r^2=0.9016, P<0.0001) is not significantly different from that expected if actual turn size equalled the expected turn size.

located posteriorly, almost in the middle of the fish's body length, at a relative distance of 47±1% from the snout (mean ± s.d., normalized to body length *BL*).

Kinematic analysis

Responses were recorded from above at 500 frames s^{-1} using a high-speed digital video system (NAC Hotshot 1280, NAC Europe, Stuttgart, Germany; resolution 1280×1024 pixels, shutter speed set to 1/500 s, lens Nikkor 35 mm 1:1.4) that monitored a sufficiently large area (about 40 cm×50 cm) in which the school initiated responses. The system allowed recordings under normal room illumination, but the bottom of the tank was diffusely illuminated from below (100 W lamp with diffuser) for better contrast. For the analyses of this study coordinates of the snout, caudal peduncle and a third point on the midline of the fish's rigid anterior body part were manually digitized using Object Image 2.12 (by Norbert Vischer, University of Amsterdam, based on NIH Image 1.63) (Fig. 3). The third point was selected as distant as possible from the snout so that its connection to the tip of the mouth coincided with the midline of the anterior body. Two additional points on the midline of the fish's posterior body part were digitized when the fish were bent but were not used in the present analysis.

The responding fish started from stationary positions directly beneath the water surface. Initially the fish were generally inclined with respect to the water surface. In order to restrict errors due to the pitched orientation we restricted the present analysis to responses in which fish were inclined by an angle of less than 45°. To do so the initial inclination in each start was calculated from how much the apparent body length of a responding fish deviated from its true body length (measured when the fish was horizontal). Allowing an initial inclination of up to 45° introduces an average angular error of <2.8° in stage 1 (in stage 2 the fish are already horizontal; S. Wöhl and S. Schuster, manuscript in preparation). This is close to the resolution obtained when measuring the angular changes (a 2.3° error is estimated from the standard deviation of the difference between two independent digitizations of the angular changes between successive frames) so that a 45° cut-off level was considered tolerable.

Onset of a response was easy to detect in all responses and was defined as the first frame in which movement occurred. The end of kinematic stage 1 could be unequivocally defined as the instant in which the fish's body was maximally bent (Fig. 3). The end of kinematic stage 2 and start of the subsequent take-off phase (stage 3) (Wöhl and Schuster, 2006) was defined as the time when the tail bent maximally in a direction opposite to that assumed previously at the end of stage 1 (Fig. 3). Again, defining the end of stage 2 in this way seemed appropriate and posed no problems in any of the responses.

In our analysis a simple variable turned out to be useful: We quantified the course of bending (stage 1) and straightening (stage 2) by means of the instantaneous 'chord length', the shortest distance from the snout to the posterior tip of the caudal peduncle normalized to its distance in the stretched-

straight fish (Fig. 4A). Furthermore, we measured the course of angular changes in the anterior body part, approximately from the snout to the center of mass. This can be done accurately, as illustrated in Fig. 4B, because the anterior part of archer fish is relatively stiff and the stretched-straight center of mass is placed rather posteriorly. Angular readings were sufficiently precise (about 2°, see above) to allow determination of angular speed and acceleration (Fig. 5) by means of 5-point moving linear regression analyses (Origin 7.5). Complete time courses of angular speed and angular acceleration could be reliably analyzed for most of the 110 responses analyzed in detail in this study. The maximum of angular speed (and angular acceleration) during the response could unequivocally be determined; in two-peaked curves with two distinct maxima the larger one was taken. Note that the turning rates of the head and of the CM are expected to be related (Domenici, 2001; Domenici et al., 2004), particularly because the anterior part of archer fish is rigid and because the CM-to-head direction is in line with the anterior part both initially before the start as well as during the take-off, as is perhaps best seen in the silhouettes shown in Fig. 3.

More work was needed to derive linear speed and acceleration with sufficient accuracy. This was mainly because of the rather large field we had to image. Linear speed and acceleration were derived from the successive position of the anterior body portion (as illustrated in Fig. 4C). Because the archer fish's anterior body is stiff and is followed posteriorly by the almost adjacent stretched-straight center of mass, CM, our reconstruction is equivalent to following the CM. Note, however, that this equivalence is not generally valid and holds only to the degree at which (1) the CM indeed plays its role as the center where propulsive forces are thought to act (i.e. Webb, 1978a; Domenici and Blake, 1997) and (2) only if the frame rate is large enough that CM displacement between frames is small compared to body length (which was the case in our recordings). However, the error introduced by the digitizing procedure was intolerably high for a precise determination of speed and acceleration. It could be efficiently reduced in a simple but laborious manner: each frame of a given sequence was independently digitized 3 times and the respective coordinates were averaged over the independent digitizations of the frame. This worked very well, as evident in the acceleration plots shown in Fig. 6 and the course of accumulated distance in Fig. 7C. Rare cases, in which reflected

Fig. 3. An archer fish predictive start imaged at 500 frames s^{-1}. Within 22 ms, the fish rotated its anterior body by 43.6° towards the later point of impact of a dislodged prey insect and then accelerated to a 1.225 m s^{-1} take-off speed. The silhouette of the fish is shown every 2 ms. The background color indicates the two distinct kinematic stages of the response, an initial bending phase (stage 1, dark blue) and a straightening phase (stage 2, light blue). Subsequent frames show the actual take-off. The location of the stretched-straight center of mass (CM, red asterisk) is indicated in each frame and the yellow dots show the points digitized in each frame for later analysis. The first two dots were used to define the turning angle and the position of the relatively stiff anterior body part to which the CM is adjacent.

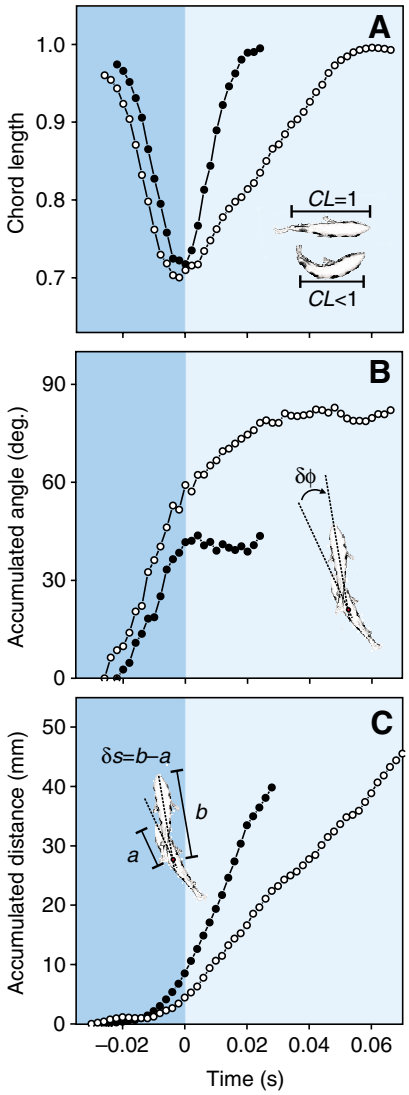

Fig. 4. Kinematics of archer fish predictive starts. Comparison of two responses (imaged at 500 frames s^{-1}) in which the fish had to execute a small turn (filled circles; response of Fig. 3) and a larger turn (open circles; frames shown in Fig. 11A). Color coding of the two kinematic stages is as in Fig. 3 with dark blue highlighting the initial bending phase and light blue indicating subsequent straightening. Time is set to zero at the start of stage 2. (A) Time course of chord length (*CL*) shows initial bending and later straightening. Inset illustrates how *CL* is defined as the minimal distance between mouth and caudal peduncle, normalized to body length. The amount of bending (i.e. the minimum *CL*) was larger for the larger turn. The courses shown are smoothed using a 5-point moving average. (B) The course of turning (accumulated angle ϕ). The inset illustrates how the angular increment δϕ was derived by lines (dotted) drawn through the anterior body portion of the fish in successive frames. The lesser turn (filled circles) already aligned the fish to the point of impact by the end of stage 1 and the angle was then kept to. In the large turn (open circles) turning continued and alignment was achieved during stage 2. (C) The accumulated displacement (*s*). The inset illustrates how the increment δ*s* between successive frames was derived. The distances (*a*, *b*) between the mouth and the point of intersection (red) of the stippled lines through the anterior body part were taken and δ*s* taken as their difference. For each frame, the mouth position was independently digitized 3 times and the average position was taken. In the two responses shown, speed values acquired in the first 20 ms after the end of stage 2 were 1.225 m s^{-1} for the lesser turn (filled circles) and 1.015 m s^{-1} for the wide-angle turn (open circles).

water droplets of the shots caused surface waves and correspondingly large frame-to-frame deviations in the apparent position of corresponding points on the fish's body, were not analyzed. The actual (large) numbers of speed and acceleration profiles that were available for analysis are reported in Table 1 and in the text.

For all responses we also evaluated the total angle of turning, between the fish's initial and take-off orientation, and the take-off speed. Total angle of turning was taken as the change in orientation between the last frame before onset of stage 1 until the last frame of stage 2. Take-off speed was determined from the distance covered during the first 20 ms that followed the last frame of stage 2.

Predictive starts

Predictive starts to dislodged prey items were elicited as described previously (Rossel et al., 2002; Wöhl and Schuster, 2006). Briefly, a dead fly (*Lucilia* sp.), in a few cases a food pellet (a Sera Cichlid stick, Sera, Heinsberg, Germany), was wetted and stuck on the lower side of a transparent cylindrical disk (Plexiglas) that was rigidly mounted so that the prey initially was at a height *h*=30 cm above the water surface. The full time course of prey motion and the point of impact were monitored in each of the responses. Besides the requirement of an initial inclination of the responding fish of less than 45°, the following criteria were applied to select the most informative responses for further analysis. (1) To ensure that only predictive starts were analyzed, responding fish clearly had to have their turns completed and to start their take-off while prey was still falling. (2) The area around the responding fish had to be free of obstacles in the interval from turn-onset to the first 20 ms after take-off. (3) To exclude the possibility that a fish could simply follow the target's motion, a minimum angle of 10° was required between the initial direction in which the fish's length axis was pointing and the direction in which the target took off. A set of *N*=76 responses was thus obtained. These showed all hallmarks of archer fish predictive starts (Rossel et al., 2002; Wöhl and Schuster, 2006): turns of various angles had to be made that accurately aligned the fish towards the later point of prey impact. This alignment was already achieved right at the beginning of the prey's falling motion and 109±62 ms (mean ± s.d.; *N*=76) before its impact. 17 of the reponses came from the shooters that had actually dislodged the prey, 59 came from bystanders. The mean error of the aim taken in the responses [sign convention as used previously (Wöhl and Schuster, 2006)] was not significantly different from zero (average –0.5°, s.d.=11.9°, *N*=76). Moreover, the fish that made the catch took off with a speed matched to both distance and time

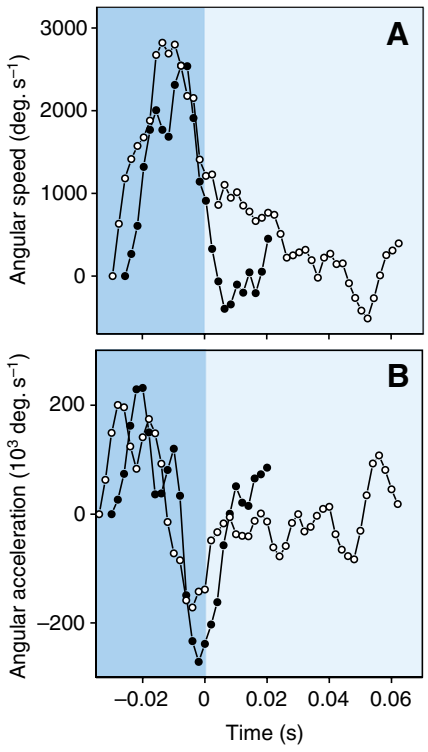

Fig. 5. Profiles of angular speed and acceleration of archer fish predictive starts. Same starts as those analyzed in Fig. 4, silhouettes of fish shown in Fig. 3 and Fig. 11A. Open circles: response with large turn (82.1°). Filled circles: response with lesser turn (43.6°). Course of angular speed $d\phi/dt$ (A) and of angular acceleration $d\phi^2/dt^2$ (B). Time zero is at start of stage 2. Background color: dark blue (stage 1), light blue (stage 2). In the lesser turn, braking at end of stage 1 was large and stage 2 angular speed approximately zero. For the larger turn angular speed was nonzero during the initial part of stage 2.

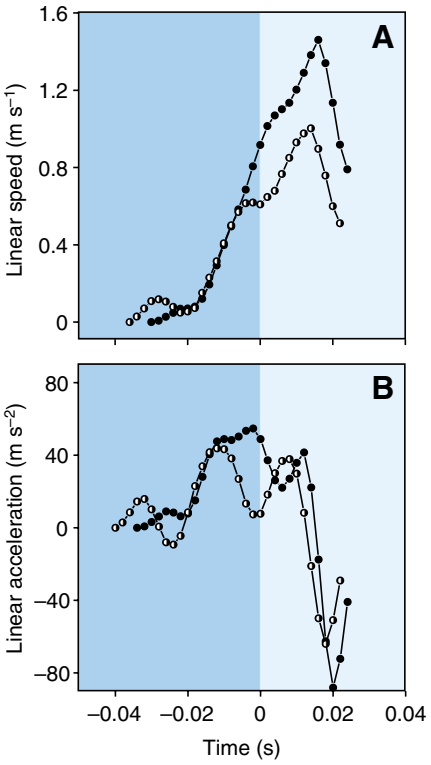

Fig. 6. Linear speed (A) and acceleration (B) profiles of archer fish predictive starts. Filled circles relate to the start shown in Fig. 3 (take-off speed 1.225 m s^{-1}, turning angle 43.6°). The half-open circles relate to a response with lesser take-off speed (0.770 m s^{-1}) but similar turning angle (39.5°). Speed and acceleration data end three frames before actual end of stage 2. This is because after that, the 5-point moving regression method used to take the derivatives causes ambiguities.

until prey impact in the way described previously [correlation between take-off speed and distance/remaining time: r^2=0.31, P<0.002 (see Wöhl and Schuster, 2006)]. Turn-sizes ranged from 4° to 156° and take-off speed ranged from 0.4 to 2.1 m s^{-1} (see Table 1). Because it does not affect any of the conclusions reached, no attempts were made to remove a weak correlation (r^2=0.104, P<0.005, N=76) that existed between the distance the responding fish had to cover and the size of the aligning turn it had to make towards the later point of impact.

Escape starts

Escape starts were difficult to elicit and fish habituated rapidly. A maximum of 10 escape-stimuli were given per day and a recovery period of at least 30 min was allowed between stimuli. Two different techniques yielded a total of 34 escape

Table 1. *Kinematics of archer fish predictive and escape starts*

	Predictive starts		Escape starts	
Variable	Range	Mean ± s.e.m. (*N*)	Range	Mean ± s.e.m. (*N*)
Stage 1 duration (ms)	12–60	25.8±1.0 (76)	12–60	27.1±2.0 (34)
Stage 2 duration (ms)	12–88	33.0±2.0 (76)	14–100	41.8±3.7 (34)
Total duration (ms)	30–146	58.8±2.8 (76)	30–144	68.9±4.8 (34)
Max. linear velocity (m s^{-1})	0.451–2.094	0.883±0.037 (69)	0.385–1.681	0.957±0.066 (33)
Max. angular velocity (deg. s^{-1})	387–4631	2 414±103 (72)	1601–4924	3433±177 (31)
Max. linear acceleration (m s^{-2})	17.3–118.4	42.8±2.2 (61)	20.3–90.1	50.7±3.6 (30)
Max. angular acceleration (deg. s^{-2})	52 982–447 646	254 554±11 568 (68)	113 014–660 660	391 251±24 511 (31)
Size of turn (deg.)	3.8–156.3	47.3±4.3 (76)	1.4–128.4	60.4±7.0 (34)
Take-off speed (m s^{-1})	0.420–2.065	1.029±0.042 (76)	0.315–2.170	0.907±0.083 (34)

C-starts for direct comparison with predictive starts. Escape starts were experimentally elicited either by sudden ejection of air bubbles from a tube mounted on the bottom of the tank below the school (15 responses) or by releasing a white styrofoam sphere (diameter 10 cm) from an initial height of 30 cm above the water surface (19 responses). In either case, the responding fish were close to the water surface, patrolling for prey, much as they were when predictive starts were elicited. The analyzed responses were selected according to various criteria: (1) a less than 45° initial inclination with respect to the water surface was required; (2) only sequences that were completed (including the first 20 ms of take-off) within the field of view of the imaging system were selected; (3) as with the predictive starts, no obstacles were allowed around the responding fish from onset of the turn till the first 20 ms after take-off; (4) responding fish had to be stationary prior to their escape start. Within the set of escapes recorded, the ranges of turning angle and of take-off speed were roughly comparable to those in the set of predictive responses. Turn-size ranged from 1.4° to 128° and take-off speed varied from 0.3 to 2.2 m s^{-1} (Table 1). Turn-size and subsequent take-off speed were not correlated (r^2=0.000, P=0.994).

Results

Archer fish predictive starts are C-starts

In contrast to expectations based on Fig. 1, the precisely aimed predictive starts of archer fish show all the hallmarks of a classic C-type fast-start. A distinct first phase (kinematic stage 1) was always seen that bends the fish's midline into the typical C-shape. This initial phase was immediately followed by a second phase (kinematic stage 2) in which the fish kicked out of the bend shape. An example of an archer fish predictive start with points digitized for further analysis is illustrated in Fig. 3. As illustrated, the stretched-straight center of mass (CM, red asterisk), the point at which propulsive forces are thought to act (Webb, 1978a), is located rather posteriorly, immediately behind the stiff anterior body part, at about half (47±1%; mean ± s.d.) of the fish's body length. Hence, the rigid anterior body part can be used as a convenient indicator of turning angle, and separating the rotational and translational shifts that occurred in the 2 ms between subsequent images could be done simply in the way illustrated in Fig. 4. In the start shown in Fig. 3, the typical bending of the fish's body into a C-shape is clearly evident, as are the two kinematic stages. In this start, the final aim was already reached by the end of kinematic stage 1 and was adhered to, while large angular changes occurred on the posterior body part of the fish as it straightened in kinematic stage 2. The time courses of body bending, accumulated angle and accumulated distance of this start are shown in Fig. 4 (filled circles). For comparison, Fig. 4 also shows the respective time courses for a second predictive start that required a larger angle of turning (open circles).

All predictive starts were of the single-bend type (*sensu* Domenici and Blake, 1997), i.e. the sense of turning was constant within each of the two stages. By the end of stage 2 the posterior part of the midline was usually (i.e. in 73 of 76 responses) very slightly bent in a direction opposing that assumed at the end of stage 1.

Performance

Although archer fish predictive starts followed the classic C-start pattern, we expected them to be either of the slow type (cf. Fig. 1) or to be compromised in other ways compared to fast C-starts of other teleost fish because of the high demands on accuracy and complex sensorimotor integration involved in the behavior. However, not only is the performance uncompromised but archer fish predictive starts are among the fastest C-type starts known: the bending into the C-shape takes less than 60 ms, in some cases only 10 ms. Also the subsequent straightening occurs within less than 88 ms, in some cases within only 12 ms. The total duration of the maneuver was always below 146 ms and could occur in as little as 30 ms. A detailed look at further kinematic variables underscores the striking performance (Table 1). Maximum angular speed was attained in the initial bending phase, on average 13±5 ms before onset of stage 2, and ranged from about 400 deg. s^{-1} to over 4500 deg. s^{-1}. The peak angular acceleration was reached very rapidly (3.0±0.7 ms; mean ± s.d., N=67) after response onset and 21.1±6.5 ms (mean ± s.d.) before the maximal bending was achieved. Angular acceleration reached impressive values of up to 450 000 deg. s^{-2}. Peak linear speed was attained 20.2±14.6 ms (mean ± s.d.) after onset of stage 2 and reached levels of up to 2.1 m s^{-1}, or 24.4 *BL* s^{-1}. The linear acceleration was up to 120 m s^{-2}, i.e. about 12× ***g*** (acceleration due to gravity).

Variability matched to the predictive task

The turns the fish had to make as well as the required speed of take-off varied substantially among our recorded responses. Turns had to be chosen in a range from 4° to 156° and take-off speed (measured as the speed attained in the first 20 ms that follow the fast-start, see Materials and methods) in a range of 0.4 to 2.1 m s^{-1}, depending on the fish's initial orientation and distance from the prey's later impact and the remaining time till impact. As expected, the kinematics of the fast-start pattern must somehow reflect this need for variability. To show the range of kinematic variations among our recorded predictive starts, Fig. 7 reports the full spectrum of time courses of three basic kinematic characteristics of the fast-starts: the bending and straightening of the fish's body (Fig. 7A), the accumulated angle of turning (Fig. 7B), and the accumulated displacement (Fig. 7C). Within the pattern of variations the following general features are worth noting: (1) the durations of the two kinematic phases are weakly correlated (r^2=0.266, P<0.0001) (Fig. 8A, red circles). (2) The rate of changes in 'chord length' (see Fig. 4A) usually tends to be symmetrical in the two kinematic stages, i.e. rapid bending of the fish's body tends to be followed by rapid straightening. However, the coupling of bending rate and straightening rate is weak (r^2=0.288, P<0.0001) (Fig. 8B,

red circles). (3) Although the major variation in the courses of accumulated angle occurs in stage 1, stage 2 also can introduce some angular variation. This was particularly evident in the large turns. In these, turning usually continued during kinematic stage 2. The stage 2 angular changes (i.e. angular deviation between end of stage 1 and end of stage 2) were in the range 5.7±16.6° (mean ± s.d., N=76). (4) The course of displacement is variable in both kinematic stages. The basic underlying pattern is a two-peaked acceleration with one peak in each stage. The height and timing of the two peaks is variable, but the peak in stage 1 is usually the larger one.

How do the variations correspond to the various turns the fish needed to make and to the required speed levels? Turn size correlated with a number of kinematic variables, for instance with stage 1 duration (r^2=0.391, P<0.0001, N=76) and stage 2 duration (r^2=0.467, P<0.0001, N=76). The best predictor of turn size was the maximum degree of body bending achieved by the end of kinematic stage 1 (r^2=0.749, P<0.0001, N=76; Fig. 9). A number of other kinematic variables correlated weakly with turn size and for many of these the correlation might come from the way in which maximum bending is achieved and subsequently released. For instance, turn size correlated with the maximum angular speed (r^2=0.382, P<0.0001, N=72) attained in the response as well as with the timing of maximal angular acceleration (r^2=0.391, P<0.0001, N=68). It correlated also with variables of linear translation, for instance with the maximal linear speed attained (r^2=0.315,

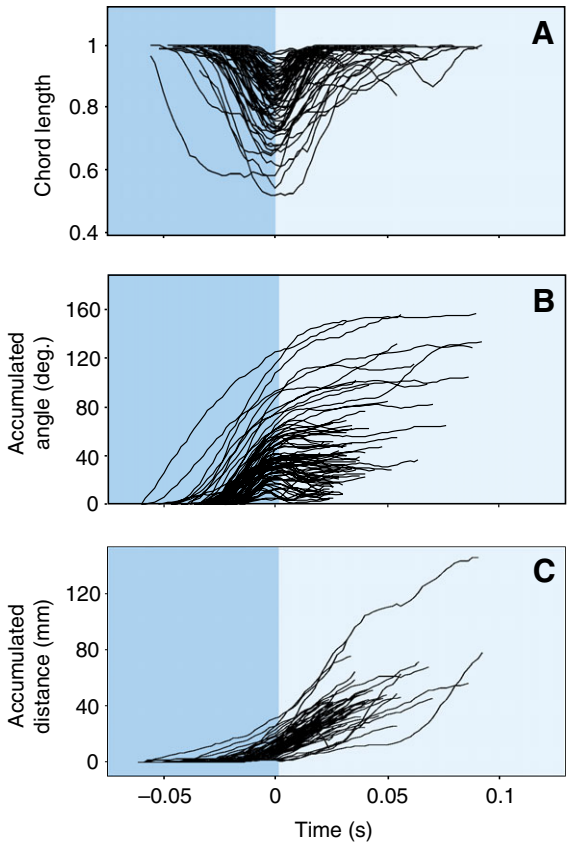

Fig. 7. The spectrum of kinematic variations among archer fish predictive fast-starts. The predictive starts required very different turns and take-off speed levels. This desired variability in the motor output should be reflected in corresponding variations in kinematics. To test this, a large number of responses (N=76) with known angles of turning and take-off speed were analyzed in detail using digital high-speed video (500 frames s^{-1}). The substantial variability among these responses is illustrated by showing (A) the course of chord length changes (CL), (B) the course of accumulated angle (ϕ) and (C) the course of accumulated displacement (s) for all starts analyzed. Variables and how they deviate for different turning angles and take-off speed are introduced in Figs 4–6, respectively. To aid comparison, time zero is set at onset of stage 2. Background color: Stage 1 dark blue, stage 2 light blue.

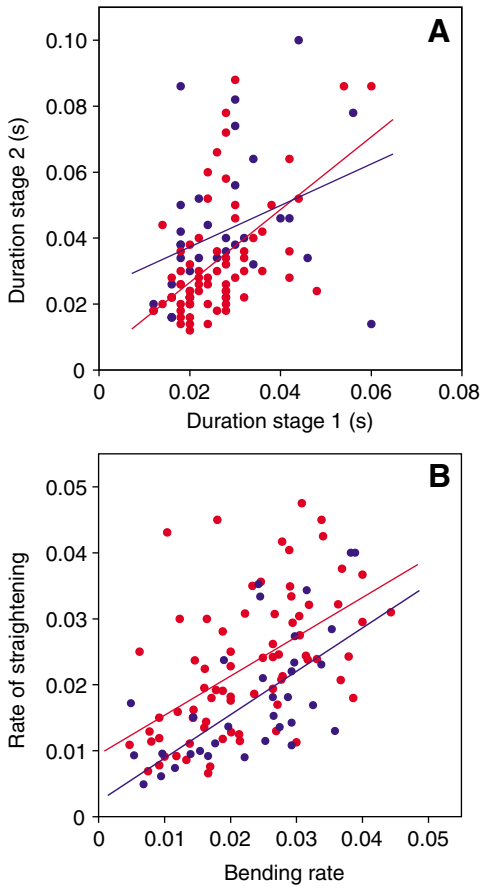

Fig. 8. Relation among kinematic stages 1 and 2 of archer fish fast-starts. Red circles relate to predictive starts, blue circles relate to escape C-starts elicited in the same group of fish. (A) Duration of stage 2 *versus* duration of stage 1. Slope and intercept of regression lines (predictive starts, red: r^2=0.319, P<0.0001, N=76; escapes, blue: r^2=0.120, P<0.05, N=34) were not different between escapes and predictive starts (P>0.05). (B) Relation of straightening rate in stage 2 (maximum of dCL/dt; CL=dimensionless chord length) to rate of bending in stage 1 (maximum of –dCL/dt). Derivatives are taken from a linear regression analysis around the point of maximum changes, using at least 5 neighboring points. Slope and intercept of regression lines (predictive starts, red: r^2=0.288, P<0.0001, N=76; escapes, blue: r^2=0.418, P<0.0001, N=34) were not different between escapes and predictive starts (P>0.05).

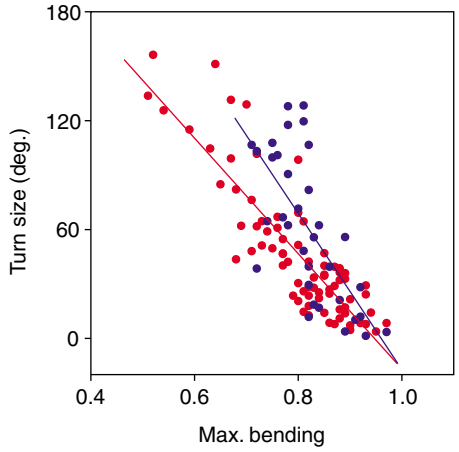

Fig. 9. Matching the fast-start to the required angle of turning. The best predictor of turn size in predictive starts (red circles) as well as in escapes (blue circles) was how much the fish's body was bent by the end of stage 1. This is quantified here as the minimum chord length (*CL*) achieved (see Fig. 4 for introduction of *CL*). Slope and intercept of the regression lines (predictive starts, red: r^2=0.749, P<0.0001, N=76; escapes, blue: r^2=0.473, P<0.0001, N=34) were not different between escapes and predictive starts (P>0.05).

P<0.0001, N=69) and its timing (r^2=0.297, P<0.0001, N=69). Larger turns did not require systematically longer initial observation of prey motion: turn size neither correlated with response latency, i.e. time from onset of prey motion till initiation of stage 1 (r^2=0.002, P=0.695, N=76), nor with time till prey impact that remained after the fish had finished stage 2 (r^2=0.009, P=0.440, N=76).

The pattern of significant correlations between kinematics and take-off speed is far less clear. Expectedly, maximal linear speed attained (r^2=0.382, P<0.0001, N=72) as well as the maximal acceleration (r^2=0.382, P<0.0001, N=72) correlated well with take-off speed. These apparently trivial correlations are still important to note, simply because they show that the fast-start kinematics is indeed of relevance for the subsequent take-off and that this is not solely determined, for instance, by fin strokes after the end of stage 2. Among the nontrivial fast-start kinematic variables that determine take-off speed the rate of straightening in stage 2 was the best predictor (r^2=0.216, P<0.0001, N=76) (Fig. 10, filled circles); however, the correlation is weak. The rate of straightening is virtually unrelated to the maximum bending achieved by the end of stage 1 (r^2=0.079, P<0.02, N=76), which was the best predictor of turn size. The correlation between the rate of straightening and the previous rate of bending (Fig. 8B) may explain two other weak correlations that existed between take-off speed and two stage 1 kinematic parameters: the rate of bending (r^2=0.156, P<0.001, N=76) and the maximum angular velocity in stage 1 (r^2=0.138, P<0.01, N=72).

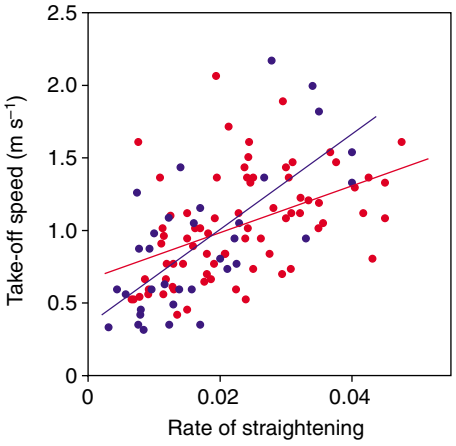

Fig. 10. Matching the fast-start to the desired take-off speed. For both predictive starts (red) and escapes (blue) take-off speed (defined as average speed within the first 20 ms subsequent to end of stage 2) correlated best with the rate of straightening during stage 2. This rate is taken as the maximum slope d*CL*/d*t* in stage 2. Slope and intercept of the regression lines (predictive starts: r^2=0.216, P<0.0001, N=76; escapes: r^2=0.484, P<0.0001, N=34) did not differ significantly between escapes and predictive starts (P>0.05).

In summary, turn size of the predictive starts seems to be set by how much the fish bends into the C-shape. The rate at which the bending is then subsequently released tends to set the speed of the subsequent take-off. But a number of other yet unclear effects are likely to contribute to take-off speed and to making speed independent of the size of the preceding turn.

Direct comparison: archer fish escape-starts

The complex and precisely aimed archer fish predictive start is evidently a typical C-type start. Comparison with C-starts of other teleost fish shows that is a top performance fast C-start (see summary of teleost fast-start patterns shown in Fig. 1). This would imply that the Mauthner-associated reticulospinal network underlies the response and, in turn, that this network is fully capable of driving a complex behavior in which flexible matching to sensory data, top speed and precision must be achieved at the same time. However, such a conclusion would be premature because two major critical issues must first be resolved: it is not known whether (1) archer fish C-type escapes do follow the pattern found in other teleost fish at all and (2) their escapes, even if they were of the C-type, would still be much faster than their predictive starts and their speed would be related to the speed of predictive starts in the same way as is the speed of a slow *versus* a fast C-start in other teleost fish. In the latter case, archer fish predictive starts, though fast compared to other teleosts, would still have to be considered as slow C-starts by archer fish standards, and this would imply that they recruit more complex circuitry than the escapes. Therefore, this section aims specifically at testing two hypotheses: (1) archer fish C-type escapes deviate from the pattern typical for teleost Mauthner-driven C-type escapes, and (2) the speed of archer fish escapes relates to that of their predictive starts in the same way as the speeds of fast and slow C-starts do in other teleost fish.

To test these hypotheses we analyzed a large number of archer fish escape starts in parallel to the characterization of

their predictive responses. This allowed us to compare, in the same group under the same conditions and with same techniques of recording and analysis, the kinematics, performance and degree of variability in archer fish predictive starts and escapes. The first hypothesis is readily falsified: all escape responses were of the C-type. No S-type escapes were observed.

Archer fish escapes share with their predictive starts a high degree of kinematic variability. The spectrum of variations in escape kinematics is documented in Fig. 11 in the same way as it was for the predictive starts in Fig. 7. The escapes reveal similar relations among stage 1 and stage 2 kinematic variables as did the predictive responses. For instance, the durations of kinematic stage 1 and 2 were weakly related (r^2=0.120, P<0.05, N=34; Fig. 8A, blue circles) and the rates of bending and subsequent straightening correlated well (r^2=0.418, P<0.0001, N=34; Fig. 8B, blue circles). Furthermore, the variations in escape kinematics could also be linked to the variations in their take-off speed and turn size. The best predictors of these variables were the same as those found for the predictive starts: turn size correlated well with the maximum bending reached by the end of stage 1 (r^2=0.473, P<0.0001, N=34) (Fig. 9, blue circles) and take-off speed correlated well with the rate of straightening in stage 2 (r^2=0.484, P<0.0001, N=34) (Fig. 10, blue circles). In none of the regression lines shown in Figs 8–10 were the slopes and y-axis intercepts different in the escapes (blue lines) and in the predictive starts (red lines).

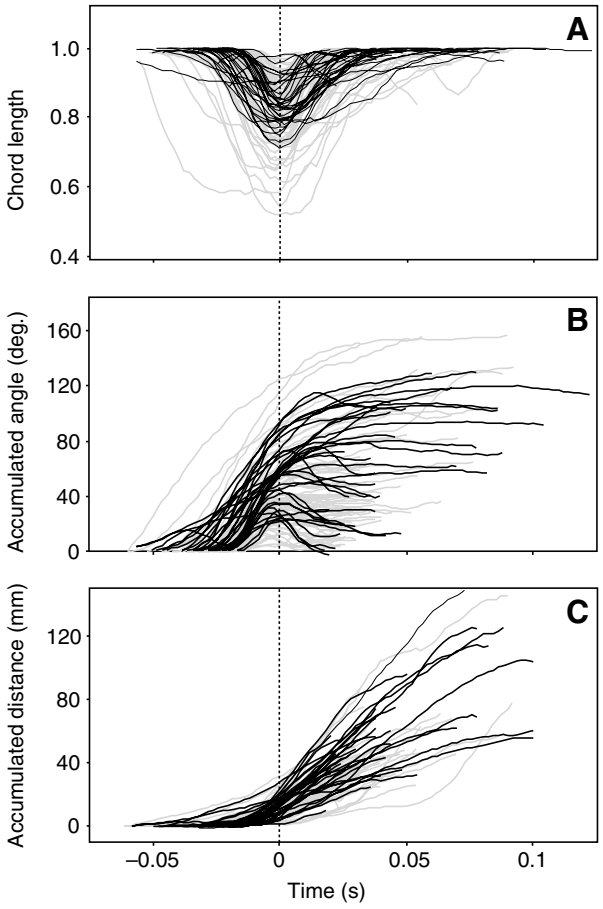

Fig. 11. The spectrum of kinematic variations among archer fish C-type escape starts. A large set of responses (N=34, black lines) from the same group used in characterizing the predictive starts was analyzed in detail using digital high-speed video (500 frames s^{-1}). The substantial variability is illustrated by showing all courses of chord length changes (CL; A), accumulated angular changes (ϕ; B) and of accumulated displacement (s; C). Time zero (dotted vertical line) is set at onset of stage 2. Variables and how they deviate for wide and narrow turns as well as for different take-off speed are introduced in Figs 4–6. The courses of the predictive starts recorded in the same group (Fig. 7) are shown for comparison (gray lines).

The kinematics of archer fish C-type escapes closely followed the pattern described in all other teleost fish studied so far and particularly that of the archer fish predictive starts described above. This is illustrated, for instance, in Fig. 12 in which a predictive start (A) and an escape start (B) are shown that both involved a similar degree of turning. The performance characteristics of archer fish C-type escapes are reported in Table 1 together with those of the predictive starts. Clearly, the performance of archer fish escapes is not superior to that of the predictive starts and, most importantly, is not related to it in the way a teleost slow C-start would be to a fast C-start. The most important conclusion that must be drawn from Table 1 is that the respective kinematic variables fully overlap. Besides their range, the table reports means ± s.e.m. for easy comparison with reports on other teleost fast starts. However, it must be emphasized that much care is needed in interpreting these averages, because the responses are variably matched to the task (which requires a certain turn and speed). Consider, for instance, the average total duration of the escapes, which was about 10 ms longer in the escapes. However, this does not mean that the total duration of archer fish escapes is in general slightly longer than that of the predictive starts. Though the ranges of turning were comparable, the average turn was slightly larger in the escapes (by about 13°) and this could account for their apparently longer average total duration. Nevertheless, even when the apparent difference in total duration – or any other apparent difference in the variables of Table 1 – was meaningful then clearly these differences are small and do not support the classification of predictive starts as slow C-starts compared to fast C-start escapes.

An interesting set of timing variables fulfilled the requirements for a MANOVA analysis and allowed a more rigorous test of whether at least the gross temporal structure of the escapes and the predictive starts must be considered identical. Fig. 13 reports how these timing variables, the timing of maximal linear speed, linear acceleration, angular speed and angular acceleration were distributed among the escapes and the predictive starts analyzed in this paper. The overlap of the respective distributions is striking and the MANOVA based on these four timing parameters detects no significant difference between escapes and predictive starts (P=0.3927). This means that the two responses are identical in terms of their temporal structure.

Fig. 12. Comparison of (A) a predictive start with (B) an escape C-start. Both starts involved similar turns and were imaged at 500 frames s^{-1}; every second frame is shown. Color of background behind fish silhouettes highlights initial bending phase (stage 1; dark blue) and propulsive phase (stage 2; light blue). An analysis of the predictive start (A) is reported in Figs 4 and 5. Take-off speed was 1.015 m s^{-1} (A) and 0.595 m s^{-1} (B) and turn size was 82.1° (A) and 99.7° (B).

In summary, the two hypotheses are clearly falsified: archer fish escapes are typical fast C-type starts and they are not faster than the predictive starts. Moreover, escapes and predictive starts are identical in terms of their temporal structure, their kinematic parameters largely overlap and their kinematics appears to be similarly adjusted to the turn the fish must make and to its intended take-off speed.

Discussion

Our results suggest that the teleost escape network is the major neuronal substrate that underlies the archer fish predictive start. This came as a surprise, because the C-start escape network was not previously noted to drive precisely aimed and yet fast feeding strikes across large distances. The competing hypothesis, that archer fish drive their predictive starts by means of another network distinct from their escape network, is difficult to reconcile with our findings. Given the arguably high costs of building and maintaining the large cells and axons that are needed in a network that performs at the high speed required in the predictive starts, it is not very likely that archer fish should need a second high-speed network for no other purpose than producing exactly the same C-type kinematics, the same degree of variability and the same performance as they already can, using their escape network. The view suggested by our findings therefore is that archer fish have found ways to modify or tune the teleost fast-start reticulospinal escape network in ways that offer the large degree of flexibility and precision needed to drive an archer fish predictive start (Fig. 2) while still maintaining the high-speed performance of the network.

Performance of escapes and predictive starts

Despite the fine-tuning of the kinematics to the turn size and speed required in the predictive task, archer fish C-starts are among the fastest known in teleost fish. Their top linear speed reaching more than 24 *BL* s^{-1} and maximum linear acceleration of up to 120 m s^{-2} (Table 1) are perhaps paralleled only by the fast-starts of pike, another acceleration specialist. In pike, direct accelerometric measurements during escapes yielded peak linear acceleration of up to 120 m s^{-2} (Harper and Blake,

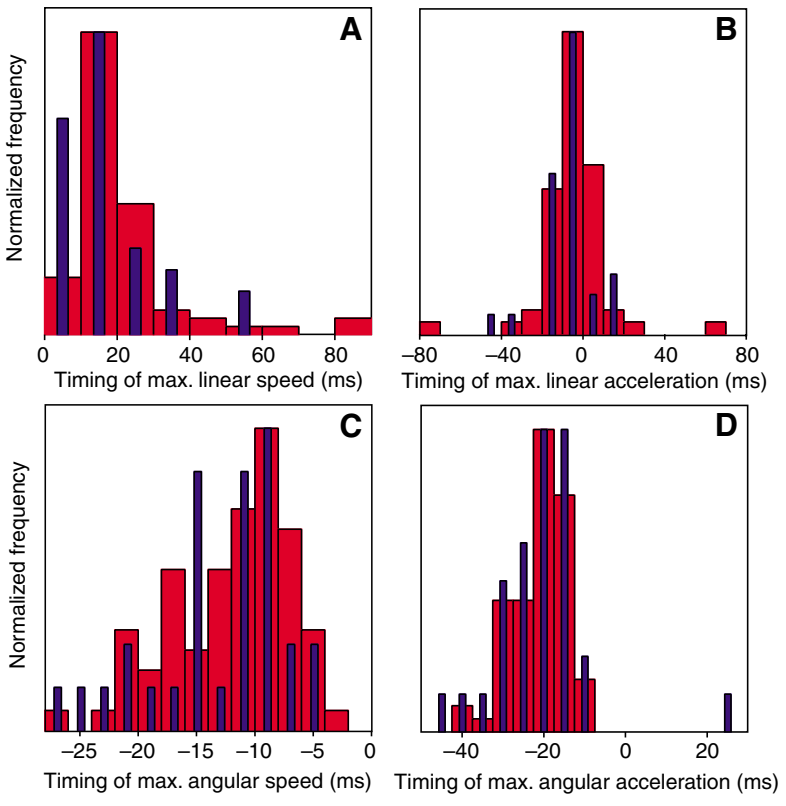

Fig. 13. Archer fish C-type escapes and predictive starts follow an identical temporal pattern. The histograms show how the timing of the maximum speed and acceleration attained was distributed among the predictive starts (red columns) and the escapes (blue columns). Time zero is at onset of stage 2. Distribution of timing of (A) maximum linear speed, (B) maximum linear acceleration, (C) maximum angular speed, and (D) maximum angular acceleration. A MANOVA detects no significant difference among these timing parameters (P=0.393). Respective bin sizes are: 10 ms (A,B), 2 ms (C), 5 ms (D). Total counts in the respective histograms were for the predictive starts N=69 (A), N=59 (B), N=72 (C), N=68 (D), and for the escapes N=33 (A), N=30 (B), N=31 (C), N=31 (D).

1991). For comparison, trout show peak linear acceleration of about 40 m s^{-2} (Webb, 1978b). The C-type escapes of pike took about twice as long as archer fish C-starts. The pike's top linear specific speed of 10.5 *BL* s^{-1} (Harper and Blake, 1991) is readily surpassed by archer fish. Part of the outstanding performance of archer fish, when compared to other acceleration specialists, might seem attributable to the higher temperatures enjoyed by archer fish. However, this seems unlikely, because a rather low Q_{10} of only 1.2 describes the temperature-dependence, for instance, of maximum speed [in trout (e.g. Johnson et al., 1996)]. At any rate, the most important point can safely be made: archer fish fast-starts are among the fastest C-type starts known in teleost fish.

The angular performance of the predictive starts is equally impressive. It is perhaps best appreciated by comparing it with the impressive performance of dipteran flies, such as *Drosophila*, whose body saccades can rotate the fly by 90° in only 50 ms (e.g. Fry et al., 2003). This implies an angular speed of 1800 deg. s^{-1} or an angular acceleration of up to about 36 000 deg. s^{-2}. By comparison, an archer fish fast start rotates the anterior body part of the fish at an angular speed up to 4500–5000 deg. s^{-1} and tops the impressive angular acceleration of the fly by at least an order of magnitude (see Table 1). Angular speed and acceleration unfortunately have not comprehensively been analyzed for many teleost fast starts. However, the evidence available suggests that archer fish predictive turns are among the fastest known in teleost fish. For the C-type escapes of an acceleration specialist, the muskellunge, Hale reports maximum angular speed values of about 2500 deg. s^{-1} and a maximum angular acceleration of 200 000 deg. s^{-2} [fig. 5 in Hale (Hale, 2002)]. For the bichir *Polypterus*, a mean maximum angular speed of 3600 deg. s^{-1} has been found (Tytell and Lauder, 2002) and a similar maximum angular speed was also in reported in goldfish (Eaton et al., 1982).

An interesting side aspect of the remarkable performance of archer fish is that their fast-starts are initiated directly beneath the water surface where the fish patrol, looking for aerial prey. It has been argued that starts performed close to the air–water interface should be energetically costly because of the energy lost to the production of surface waves (e.g. Hertel, 1966; Webb et al., 1991). In case that Hertel's original estimate of an up to fivefold drag increase close to the surface is correct, then the fast-start performance of archer fish would be even more remarkable and would seem to imply that archer fish have found efficient ways to diminish the costly surface waves during their fast-starts. The body form of archer fish seems perfectly optimized for producing powerful accelerations even against large drag. As is common among acceleration specialists, in archer fish large body depth is placed posteriorly (Webb, 1984) and the dorsal and anal fins are fully erected after stage 1, thus maximizing the amount of water that is accelerated backwards.

Using C-start circuitry to drive archer fish predictive starts

Previous work has suggested various distinct fast-start patterns that each appear to be optimized in a particular aspect (see Fig. 1). Fish could select the appropriate motor pattern depending on whether high accuracy, top acceleration or a wide range of turning angles is required. The underlying notion that seems to be supported by the range of distinct patterns is that a single program is unable to fulfil all requirements. This is very reasonable because a trade-off is likely to exist between achieving top acceleration, accuracy, a broad range of output variables (i.e. angle and speed at take-off) and a large amount of variability required in matching the motor program according to actual sensory information. Taking this perspective, the present classification of fast-starts (Fig. 1) (Domenici and Blake, 1997; Schriefer and Hale, 2004) could be understood as follows. (1) The S-start offers speed and accuracy but only limited angular range. It has therefore previously been considered the only fast-start used in hunting. (2) C-starts offer speed and a large angular range but limited accuracy. Previously no predator has been reported to use a C-type fast start and this seemed fitting with the apparently large scatter around a mean escape direction chosen for a fixed stimulus position. (3) Most tellingly, fish that do perform fast C-starts have been found to resort to a slower form when high accuracy is required. This slower form probably involves more neurones of the reticulospinal network (Domenici and Batty, 1997; Domenici and Blake, 1997) and has been described as a slow C-type start that combines large angular range and accuracy but allows only reduced speed.

The particular situation faced by hunting archer fish is not easily fulfilled by any of these three known patterns. The wide angular range required of the response seems to exclude the precise S-type pattern and, combined with the precision needed, would only allow for a slow C-type start. However, the predictive starts must be fast. This is because of (1) the competition within their own school, (2) the risk of an escape of the downed insect and (3) the heavy pressure from other surface-feeding fish whose mechanosensory system is immediately alarmed (e.g. Bleckmann, 1993) as soon as the prey actually impacts the surface. In fact, juvenile (surface-feeding) belonid fish are usually found together with archer fish in various biotopes in Thailand, outnumbering the archer fish so greatly (S. Schuster, unpublished) that these would appear to have little chance of making a catch unless they are already on their way long before the belonids are alarmed.

Matching the motor pattern to the initial values of prey movement

The advent of digital high-speed video has enabled researchers to analyze a large number of fast-starts in detail and this has disposed of the earlier views (e.g. Webb, 1976; Eaton et al., 1977) that fast-starts are partly stereotypic. Our results, together with those of others (e.g. Tytell and Lauder, 2002), clearly demonstrate how extremely variable a C-type fast start can be in both of its two kinematic stages. The defined neuroethological context of archer fish predictive starts (see Fig. 2) may be helpful in showing that these variations are not simply 'noise' within the motor system, but rather are the adjustments by which the fish tune fast-start kinematics to the

task, i.e. set specific initial speed levels and turn angles. The findings may contribute to the understanding that characterizing an 'average' fast-start performance may be of little use unless the 'desired' motor output (i.e. the turning angle and take-off speed) is known.

An interesting detail of archer fish predictive starts is that the angle of turning must not be coupled to the take-off speed. How can this be realized in a C-type start? The problem here is that a large bend is needed for a large turn. But kicking out of strong bending should then lead to high acceleration and high take-off speed so that larger turns would also lead to large take-off speed. How are the two variables decoupled? To do this archer fish appear to modulate the speed at which a given degree of bending is released. Lower take-off speed from a given state of bending is achieved by lowering the rate of straightening.

Implications for reticulospinal control

The finding that predictive starts are fast C-starts implies that the underlying small network of paired identified reticulospinal neurons is in principle capable of the rather complex high-speed processing required to drive the predictive responses. At present it is a wide open question which specific neuronal computations contribute to the required precision and tuning and how the input structure (or the recruitment of different parts of the system) would decide the obviously different directionality of escapes and feeding starts. It comes as no surprise, however, that the network does hold an enormous computational potential that could be used in the task. Of these we would like to emphasize three aspects.

(1) Dendritic integration. The wide dendritic integration fields of the Mauthner cells and their serial homologues are suited to integrating a multiplicity of inputs in yet unknown ways. Moreover, each cell receives inputs *via* both chemical and electrical synapses, which adds to the richness of possible computations.

(2) Distributed processing. While firing of the Mauthner cell usually appears to elicit the C-type start in intact fish, it has long been known that the start can also be elicited in the absence of the Mauthner cell. This suggests distributed processing that also involves the other cells and in which missing cells can be partly substituted by the remaining ones. The first study to suggest this was, to our knowledge, by Kimmel et al. (Kimmel et al., 1980). Using developmental deletions in embryonal zebrafish this study showed that zebrafish without Mauthner cells are capable of fast-start with no reduction in latency but with a slightly reduced performance. In goldfish, Eaton et al. (Eaton et al., 1982) found fast-starts of equal performance but longer latency after the Mauthner cells had been destroyed. Perhaps most telling are results of *in vivo* laser ablation in larval zebrafish (Liu and Fetcho, 1999). This study showed significant increases in response latency and a striking decrease in performance only if the Mauthner cells are killed together with the two largest segmentally related (Mauthner like) hindbrain cells (called MiD2cm and MiD3cm) (Liu and Fetcho, 1999) (see also Fetcho and Higashijima, 2004). It is therefore clear that distributed processing occurs in the segmentally related hindbrain cells but the various functional roles of the distributed processing remain to be seen.

(3) Downstream adjustments. A third aspect of potential relevance is the fine-tuning that can probably be done downstream at the level of the motoneurones. Even after dendritic integration of sensory inputs and distributed processing in the network has led to issuing a fast-start command there is still plenty of room for complex adjustments. An interesting possibility, raised by the findings of an early study (Aljure et al., 1980), is that other synaptic inputs to the motoneurons could preset their state to achieve precise control over angle and speed.

Conclusions

The findings presented here have two major implications. (1) It is clear that the teleost C-start network of identified reticulospinal neurons is capable of driving even rather complex behaviors, such as the archer fish predictive start, that require a high degree of precision and complex sensomotor integration performed accurately and at top speed. (2) The accessibility of this network, in turn, offers the fascinating perspective of disclosing in the future how a defined vertebrate network of a small number of identified neurons performs an impressively complex sensomotor integration task and is tuned to do so.

It is a pleasure to thank Burkhard Pfeiffer for thoroughly guiding us through statistics, Peter Übel for various constructions, Iris Schindler for helping us check the accuracy of the kinematic variables and our referees for their many stimulating and helpful comments on the manuscript. We gratefully acknowledge generous support of this work by the Deutsche Forschungsgemeinschaft.

References

Aljure, E., Day, J. W. and Bennett, M. V. L. (1980). Postsynaptic depression of Mauthner cell-mediated startle reflex, a possible contributor to habituation. *Brain Res.* **188**, 261-268.

Bennett, M. V. L. (1984). Escapism: some startling revelations. In *Neural Mechanisms of Startle Behavior* (ed. R. C. Eaton), pp. 353-363. New York: Plenum.

Bleckmann, H. (1993). Role of the lateral line in fish behavior. In *Behavior of Teleost Fishes* (ed. T. J. Pitcher), pp. 201-246. London: Chapman & Hall.

Buchanan, J. T. (1993). Electrophysiological properties of identified classes of lamprey spinal neurons. *J. Neurophysiol.* **70**, 2313-2325.

Deliagina, T. G., Zelenin, P. V., Fagerstedt, P., Grillner, S. and Orlovsky, G. N. (2000). Activity of reticulospinal neurons during locomotion in the freely behaving lamprey. *J. Neurophysiol.* **83**, 853-863.

Dill, L. M. (1977). Refraction and the spitting behavior of the archerfish (*Toxotes chatareus*). *Behav. Ecol. Sociobiol.* **2**, 169-184.

Domenici, P. (2001). Scaling the locomotor performance in predator-prey interactions: from fish to killer whales. *Comp. Biochem. Physiol.* **131A**, 169-182.

Domenici, P. and Batty, R. S. (1997). The escape behavior of solitary herring and comparisons with schooling individuals. *Mar. Biol.* **128**, 29-38.

Domenici, P. and Blake, R. W. (1993). Escape trajectories in angelfish (*Pterophyllum eimekei*). *J. Exp. Biol.* **177**, 253-272.

Domenici, P. and Blake, R. W. (1997). The kinematics and performance of fish fast-start swimming. *J. Exp. Biol.* **200**, 1165-1178.

Domenici, P., Standen, E. M. and Levine, R. P. (2004). Escape manoeuvres in the spiny dogfish (*Squalus acanthias*). *J. Exp. Biol.* **207**, 2339-2349.
Eaton, R. C. and Emberley, D. S. (1991). How stimulus direction determines the trajectory of the Mauthner-initiated escape response in a teleost fish. *J. Exp. Biol.* **161**, 469-487.
Eaton, R. C., Bombardieri, R. and Meyer, D. L. (1977). The Mauthner-initiated startle response in teleost fish. *J. Exp. Biol.* **66**, 65-81.
Eaton, R. C., Lavender, W. A. and Wieland, C. M. (1982). Alternative neural pathways initiate fast-start responses following lesions of the Mauthner neuron in goldfish. *J. Comp. Physiol.* **145**, 485-496.
Eaton, R. C., Lee, R. K. K. and Foreman, M. B. (2001). The Mauthner cell and other identified neurons of the brainstem escape network of fish. *Prog. Neurobiol.* **63**, 467-485.
Faber, D. S., Fetcho, J. R. and Korn, H. (1989). Neuronal networks underlying the escape response in goldfish: general implications for motor control. *Ann. N. Y. Acad. Sci.* **563**, 11-33.
Fetcho, J. R. and Bhatt, D. H. (2004). Genes and photons: new avenues into the neuronal basis of behavior. *Curr. Opin. Neurobiol.* **14**, 707-714.
Fetcho, J. R. and Higashijima, S. I. (2004). Optical and genetic approaches toward understanding neuronal circuits in zebrafish. *Integr. Comp. Biol.* **44**, 57-70.
Fetcho, J. R. and O'Malley, D. M. (1997). Imaging neuronal networks in behaving animals. *Curr. Opin. Neurobiol.* **7**, 832-838.
Foreman, M. B. and Eaton, R. C. (1993). The direction change concept for reticulospinal control of goldfish escape. *J. Neurosci.* **13**, 4101-4133.
Fry, S. N., Sayaman, R. and Dickinson, M. D. (2003). The aerodynamics of free-flight maneuvers in Drosophila. *Science* **300**, 495-498.
Hale, M. E. (2002). S- and C-start escape responses of the muskellunge (*Esox masquinongy*) require alternative neuromotor mechanisms. *J. Exp. Biol.* **205**, 2005-2016.
Hale, M. E., Long, J. H., McHenry, M. J. and Westneat, M. W. (2002). Evolution of behavior and neural control of the fast-start escape response. *Evolution* **56**, 993-1007.
Hale, M. E., Kheirbek, M. A., Schriefer, J. E. and Prince, V. E. (2004). *Hox* Gene misexpression and cell-specific lesions reveal functionality of homeotically transformed neurons. *J. Neurosci.* **24**, 3070-3076.
Harper, D. G. and Blake, R. W. (1990). Fast-start performance of rainbow trout *Salmo gairdneri* and northern pike *Esox lucius*. *J. Exp. Biol.* **150**, 321-342.
Harper, D. G. and Blake, R. W. (1991). Prey capture and the fast-start performance of northern pike *Esox lucius*. *J. Exp. Biol.* **155**, 175-192.
Hertel, H. (1966). *Structure, Form and Movement*. New York: Reinhold.
Johnson, T. P., Bennett, A. F. and McLister, J. D. (1996). Thermal dependence and acclimation of fast start locomotion and its physiological basis in rainbow trout (*Oncorhynchus mykiss*). *Physiol. Zool.* **69**, 276-292.
Kimmel, C. B., Eaton, R. C. and Powell, S. L. (1980). Decreased fast-start performance of zebrafish lacking Mauthner neurons. *J. Comp. Physiol.* **140**, 343-350.
Liu, K. S. and Fetcho, J. R. (1999). Laser ablations reveal functional relationships of segmental hindbrain neurons in zebrafish. *Neuron* **23**, 325-335.
Lüling, K. H. (1963). The archerfish. *Sci. Am.* **209**, 100-108.
McClellan, A. D. and Grillner, S. (1983). Initiation and sensory gating of 'Fictive' swimming and withdrawal responses in an *in vitro* preparation of the lamprey spinal cord. *Brain Res.* **269**, 237-250.
Miesenböck, G. (2004). Genetic methods for illuminating the function of neural circuits. *Curr. Opin. Neurobiol.* **14**, 395-402.
Nissanov, J. and Eaton, R. C. (1989). Reticulospinal control of rapid escape turning maneuvers in fishes. *Am. Zool.* **29**, 103-121.
O'Malley, D. M., Kao, Y.-H. and Fetcho, J. R. (1996). Imaging the functional organization of zebrafish hindbrain segments during escape behaviors. *Neuron* **17**, 1145-1155.
O'Steen, S., Cullum, A. J. and Bennett, A. F. (2002). Rapid evolution of escape performance in Trinidadian guppies (*Poecilia reticulata*). *Evolution* **56**, 776-784.
Rossel, S., Corlija, J. and Schuster, S. (2002). Predicting three-dimensional target motion: how archer fish determine where to catch their dislodged prey. *J. Exp. Biol.* **205**, 3321-3326.
Schlegel, T., Schmid, C. J. and Schuster, S. (2006). Archerfish shots are evolutionarily matched to prey adhesion. *Curr. Biol.* **16**, R836-R837.
Schriefer, J. E. and Hale, M. E. (2004). Strikes and startles of northern pike (*Esox lucius*): a comparison of muscle activity and kinematics between S-start behaviors. *J. Exp. Biol.* **207**, 535-544.
Schuster, S., Rossel, S., Schmidtmann, A., Jäger, I. and Poralla, J. (2004). Archer fish learn to compensate for complex optical distortions to determine the absolute size of their aerial prey. *Curr. Biol.* **14**, 1565-1568.
Schuster, S., Wöhl, S., Griebsch, M. and Klostermeier, I. (2006). Animal cognition: how archer fish learn to down rapidly moving prey. *Curr. Biol.* **16**, 378-383.
Spierts, I. L. Y. and van Leeuwen, J. L. (1999). Kinematics and muscle dynamics of C- and S-starts of carp (*Cyprinus carpio*, L.). *J. Exp. Biol.* **202**, 393-406.
Tytell, E. D. and Lauder, G. V. (2002). The C-start escape response of *Polypterus senegalus*: bilateral muscle activity and variation during stage 1 and 2. *J. Exp. Biol.* **205**, 2591-2603.
Webb, P. W. (1975). Acceleration performance of rainbow trout, *Salmo gairdneri*, and green sunfish, *Lepomis cyanellus*. *J. Exp. Biol.* **74**, 211-226.
Webb, P. W. (1976). The effect of size on the fast-start performance of rainbow trout *Salmo gairdneri*, and a consideration of piscivorous predator-prey interactions. *J. Exp. Biol.* **65**, 157-177.
Webb, P. W. (1978a). Fast-start performance and body form in seven species of teleost fish. *J. Exp. Biol.* **74**, 211-226.
Webb, P. W. (1978b). Temperature effects on acceleration of rainbow trout *Salmo gairdneri*. *J. Fish. Res. Bd Can.* **35**, 1417-1422.
Webb, P. W. (1984). Body form, locomotion and foraging in aquatic vertebrates. *Am. Zool.* **24**, 107-120.
Webb, P. W., Sims, D. and Schultz, W. W. (1991). The effects of an air/water surface on the fast-start performance of rainbow trout (*Oncorhynchus mykiss*). *J. Exp. Biol.* **155**, 219-226.
Weihs, D. (1973). The mechanisms of rapid starting of slender fish. *Biorheology* **10**, 343-350.
Westneat, M. W., Hale, M. E., McHenry, M. J. and Lang, J. H. (1998). Mechanics of the fast-start: muscle function and the role of intramuscular pressure in the escape behavior of *Amia calva* and *Polypterus palmas*. *J. Exp. Biol.* **201**, 3041-3055.
Wöhl, S. and Schuster, S. (2006). Hunting archer fish match their take-off speed to distance from the future point of catch. *J. Exp. Biol.* **209**, 141-151.
Zottoli, S. J. (1977). Correlation of the startle reflex and Mauthner cell auditory responses in the unrestrained goldfish. *J. Exp. Biol.* **66**, 243-254.
Zottoli, S. J. and Faber, D. S. (2000). The Mauthner cell: what has it taught us? *Neuroscientist* **6**, 25-37.